

# 1 Close-Coupling Time-Dependent Quantum Dynamics Study of the H + HCl Reaction

2 Li Yao,<sup>†,‡</sup> Ke-Li Han,<sup>\*,†</sup> He-Shan Song,<sup>\*,‡</sup> and Dong-Hui Zhang<sup>§</sup>

3 *Center for Computational Chemistry and State Key Laboratory of Molecular Reaction Dynamics,*  
 4 *Dalian Institute of Chemical Physics, Chinese Academy of Sciences, Dalian 116023, China, Department of*  
 5 *Physics, Dalian University of Technology, Dalian 116023, China, and Department of Computational Science,*  
 6 *National University of Singapore, Singapore*

7 *Received: September 24, 2002; In Final Form: February 15, 2003*

8 The paper presents a theoretical study of the dynamics of the H + HCl system on the potential energy surface  
 9 (PES) of Bian and Werner (Bian, W.; Werner, H. -J., *J. Chem. Phys.* 2000, 112, 220). A time-dependent  
 10 wave packet approach was employed to calculate state-to-state reaction probabilities for the exchanged and  
 11 abstraction channels. The most recent PES for the system has been used in the calculations. Reaction  
 12 probabilities have also been calculated for several values of the total angular momentum  $J > 0$ . Those have  
 13 then been used to estimate cross sections and rate constants for both channels. The calculated cross sections  
 14 can be compared with the results of previous quasiclassical trajectory calculations and reaction dynamics  
 15 experimental on the abstraction channel. In addition, the calculated rate constants are in the reasonably good  
 16 agreement with experimental measurement.

## 1. Introduction

18 The gas-phase reaction of H + HCl and the corresponding  
 19 reverse reaction of Cl atoms with molecular H represent  
 20 important elementary steps in the  $H_2 + Cl_2 \rightarrow 2HCl$  reaction  
 21 system, which has played a major role in the development of  
 22 chemical kinetics and to the environment in atmospheric  
 23 chemistry.<sup>1,2</sup> A large number of kinetics studies were carried  
 24 out for the H + HCl elementary reaction in the temperature  
 25 range  $195 K \leq T \leq 1200 K$ ,<sup>3</sup> including experiments in which the  
 26 influence of selective vibrational excitation of HCl on the  
 27 reaction rate was investigated.<sup>4-8</sup> Recent studies<sup>9-16</sup> of the  
 28 reaction H + HCl at a collision energy of 1.6 eV have measured  
 29 the integral cross section for the abstraction channel to be  $(2 \pm 1)$   
 30  $\text{\AA}^2$ ,<sup>9,10</sup> where as the exchange plus energy-transfer channels gave  
 31 a combined cross section of  $(13 \pm 3) \text{\AA}^2$ .<sup>9,10</sup> It has been shown  
 32 by Wight et al.<sup>11</sup> that the dominant process is energy transfer.<sup>2</sup>  
 33 In contrast to numerous experiments, only a few theoretical  
 34 studies have been reported for this H + HCl reaction.

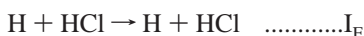
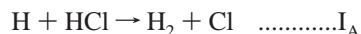
35 Due to the relatively low collision energies employed in the  
 36 Cl + H<sub>2</sub> dynamics experiments, these studies provided detailed  
 37 information about the region of the HClH potential energy  
 38 surface (PES) close to the threshold of reaction.<sup>17-23</sup> However,  
 39 much less information is available concerning the high-energy  
 40 regions of the PES that can be assessed in H + HCl dynamics  
 41 experiments using translationally excited H atoms.<sup>24-27</sup> The first  
 42 globally realistic Cl-H-H PES was calculated by Baer and  
 43 Last,<sup>26</sup> and a more recent PES was published by Truhlar et al.<sup>27</sup>  
 44 Therefore, a scaled PES has been computed by Bian and Werner  
 45 (BW2)<sup>28</sup> to get the dissociation energies right. The H<sub>2</sub>Cl reaction  
 46 system was presented by Bian et al.<sup>28</sup> more recently. The PES  
 47 was developed using the highly accurate electronic structure  
 48 methods based on extensive ab initio calculations and very large  
 49 basis sets presently applied. The ab initio calculations were

50 carried out at more than 1200 nuclear geometries.<sup>28</sup> The later  
 51 version of the BW2 PES was further improved by scaling the  
 52 correlation energies at all geometries with a constant factor.<sup>28</sup>

53 A major theoretical problem stems from the inability of  
 54 current ab initio and semiempirical methods in providing a  
 55 reliable PES. Recently, Aoiz et al.<sup>29,30</sup> have carried out quasi-  
 56 classical trajectory (QCT) calculations on two versions of the  
 57 BW2 PES for the reaction.<sup>30</sup> The calculated cross sections are  
 58 in reasonably good agreement with experimental measurement.  
 59 This provides some assurance that the BW2 PES may be  
 60 reasonably accurate near the transition state. To the best of our  
 61 knowledge, no time-dependent wave packet (TDWP) study for  
 62 the reaction system corresponding to a collision energy range  
 63 of [0.1, 1.4] eV was reported on the BW2 PES.

64 In the present work, the reaction probabilities have been  
 65 calculated by employing TDWP method for several values of  
 66 the total angular momentum quantum number  $J > 0$  on BW2  
 67 PES. Those have then been used to estimate cross sections and  
 68 rate constants for both channels. The calculated cross sections  
 69 can be compared with the results of previous QCT calculations  
 70 and reaction dynamics experiments of Aoiz et al.<sup>30</sup> and  
 71 experiments of Brownsword et al.<sup>25</sup> on the abstraction channel.  
 72 The thermal rate constants of HCl are calculated by employing  
 73 the uniform  $J$ -shifting method,<sup>32,33</sup> and a comparison with  
 74 experimental measurement is provided.

75 In this paper, we have carried out TDWP calculations for  
 76 the following two channels of the H + HCl reaction



77 to figure out the different dynamical properties of the  $I_A$   
 78 abstraction channel, the  $I_E$  exchange channel.

79 This paper is organized as follows: Section 2 gives a brief  
 80 review of the theoretical methodologies used in the current  
 81 study. The result of numerical calculation and discussion of the  
 82 result are given in Section 3. Comparisons with other theoretical

\* Corresponding authors: E-mail: klhan@ms.dicp.ac.cn.

† Dalian Institute of Chemical Physics, Chinese Academy of Sciences.

‡ Dalian University of Technology.

§ National University of Singapore.

83 calculations and with experimental measurement, whenever  
84 possible, are also given in this section. Section 4 concludes the  
85 article.

## 86 2. Theory

87 Here, we briefly describe the TDWP method employed to  
88 calculate the initial state-selected total reaction probability with  
89 the final resolved products. The reader is referred to ref 34 for  
90 more detailed discussions of the methodology. In the present  
91 study, we solve the time-dependent Schrödinger equation

$$92 i\hbar \frac{\partial \Psi}{\partial t} = H\Psi \quad (1)$$

92 for the H + HCl reaction. The Hamiltonian expressed in the  
93 reactant Jacobi coordinates for a given total angular momentum  
94 quantum number  $J$  can be written as

$$95 H = -\frac{\hbar^2}{2\mu_r} \frac{\partial^2}{\partial R^2} + \frac{(\vec{J} - \vec{j})^2}{2\mu_r R^2} + \frac{\vec{j}^2}{2\mu_r r^2} + V(\vec{r}, \vec{R}) + h(r) \quad (2)$$

95 where  $\vec{r}$  is the diatom internuclear,  $\vec{R}$  is the vector jointing the  
96 center of mass of diatom to the atom, while  $\mu_r$  is the reduced  
97 mass for HCl, and  $\mu_R$  is the reduced mass between H and HCl.  
98  $\vec{J}$  and  $\vec{j}$  represent the total angular momentum operator and the  
99 rotational angular momentum operator of HCl, respectively.  
100  $V(\vec{r}, \vec{R})$  is the interaction potential excluding the diatomic  
101 potential of the diatom. The diatomic reference Hamiltonian  
102  $h(r)$  is defined as

$$103 h(r) = -\frac{\hbar^2}{2\mu_r} \frac{\partial^2}{\partial r^2} + V_r(r) \quad (3)$$

103 where  $V_r(r)$  is a diatomic reference potential.

104 The time-dependent wave function satisfying the Schrödinger  
105 eq 1 can be expanded in terms of the body-fixed translational–  
106 vibrational–rotational basis, defined using the reactant Jacobi  
107 coordinates, as<sup>35</sup>

$$108 \Psi_{v_0j_0K_0}^{JM\epsilon}(\vec{R}, \vec{r}, t) = \sum_{n, v, j, K} F_{nvjK, v_0j_0K_0}^{JM\epsilon}(t) u_n^v(R) \phi_{jv}(r) Y_{jK}^{JM\epsilon}(\hat{R}, \hat{r}) \quad (4)$$

108 where  $n$  is the translational basis label and  $M$  and  $K$  are the  
109 projection quantum numbers of  $J$  on the space-fixed  $z$  axis and  
110 body-fixed  $z$  axis, respectively.  $(v_0, j_0, K_0)$  denotes the initial  
111 rovibrational state, and  $\epsilon$  is the parity of the system defined as  
112  $\epsilon = (-1)^{j+L}$  with  $L$  being the orbital angular momentum  
113 quantum number. The reader can find the definitions of various  
114 basis functions elsewhere.<sup>34</sup>

115 The split-operator method<sup>36</sup> is employed to carry out the wave  
116 packet propagation. The time-dependent wave function is  
117 absorbed at the edges of the grid area to avoid artificial  
118 reflections.<sup>37</sup> Finally the initial state-selected total (final-state-  
119 summed) reaction probabilities are obtained through the flux  
120 calculation<sup>35</sup> at the end of the propagation.

$$121 P_{v_0j_0K_0}^J(E) = \langle \psi_{v_0j_0K_0}^{JM\epsilon+}(E) | \frac{1}{2} [\delta(\hat{s} - s_0) \hat{v}_s + \hat{v}_s \delta(\hat{s} - s_0)] | \psi_{v_0j_0K_0}^{JM\epsilon+}(E) \rangle \quad (5)$$

121 where  $s$  is the coordinate perpendicular to a surface located at  
122  $s_0$  for flux evaluation and  $v_s$  is the velocity operator corresponding  
123 to the coordinate  $s$ .  $\psi_{v_0j_0K_0}^{JM\epsilon+}(E)$  is the time-independent  
124 wave function that can be obtained by Fourier transforming the  
125 TDWP wave function.

Once the reaction probabilities  $P_{v_0j_0K_0}^J(E)$  have been calculated for all fixed angular momenta  $J$ , calculation for the cross sections and rate constants are straightforward. The cross section is given by

$$126 \sigma_{v_0j_0}(E) = \frac{\pi}{k_{v_0j_0}^2} \sum_J (2J + 1) P_{v_0j_0}^J(E) \quad (6)$$

127 where  $k_{v_0j_0} = (2\mu_R E)^{1/2}/\hbar$  is the wavenumber corresponding to  
128 the initial state at fixed collision energy  $E$ , and  $P_{v_0j_0}^J(E)$  is given  
129 by

$$130 P_{v_0j_0}^J(E) = \frac{1}{2j_0 + 1} \sum_{K_0} P_{v_0j_0K_0}^J(E) \quad (7)$$

133 In practice, we can use the interpolation method to get the  
134 probabilities for missing values of  $J$ ; reaction probabilities at  
135 only a limited number of total angular momentum values of  $J$   
136 need to be explicitly calculated.

137 As in refs 34, 38, we construct wave packets and propagate  
138 them to calculate the reaction probabilities for  $P^J(E)$  each  
139 product. The integral cross section from a specific initial state  
140  $j_0$  is obtained by summing the reaction probabilities over all  
141 the partial waves on total angular momentum.

142 The rate constants are calculated for the initial states ( $v = 0$ ,  
143  $j = 0$ ) of HCl by using the uniform version<sup>32</sup> of  $J$ -shifting  
144 approximation.<sup>33</sup> The initial state-specific thermal rate constant  
145 in the uniform  $J$ -shifting scheme is given as

$$146 K(T) = \sqrt{\frac{2\pi}{(\mu_R k_B T)^3}} Q^0(T) \sum_J (2J + 1) e^{-B_J(T)J(J+1)/k_B T} \quad (8)$$

146 The shifting constant is determined by<sup>32</sup>

$$147 B_J(T) = \frac{k_B T}{J(J+1) - J_i(J_i+1)} \ln \left( \frac{Q^{J_i}}{Q^J} \right) \quad (9)$$

147 where  $k_B$  is the Boltzmann constant,  $T$  is the temperature, and  
148  $Q^{J_i}$  is a partitionlike function defined as

$$149 Q^J = \int P^J(E) e^{-E/k_B T} dE \quad (10)$$

150 where  $P^J(E)$  is the probabilities for a total angular momentum  
151 from a given initial state.

152 The numerical parameters for the wave packet propagation  
153 are as follows: A total number of 200 sine functions (among  
154 them 80 for the interaction region) are employed for the  
155 translational coordinate  $R$  in a range of [0.8, 14.0]  $a_0$ . A total of  
156 100 vibrational functions are employed for  $r$  in the range of  
157 [0.8, 8.5]  $a_0$  for the reagents HCl in the interaction region. For  
158 the rotational basis, we use  $j_{\max} = 45$ . The number of  $K$  used in  
159 our calculation is given by  $K_{\max} = \max(3, K_0 + 2)$  starting with  
160  $K_0 = 0$ . The largest number of  $K$  used is equal to 6 for the  $j = 0$ ,  
161  $K_0 = 0$  initial state (for  $\epsilon = -1$ , there is one less  $K$  block  
162 used). These values of  $K_0$  and  $K_{\max}$  were determined following  
163 an extensive series of tests.<sup>35</sup> It was found that convergence of  
164 total cross sections, for all the reported initial (rotational) states  
165

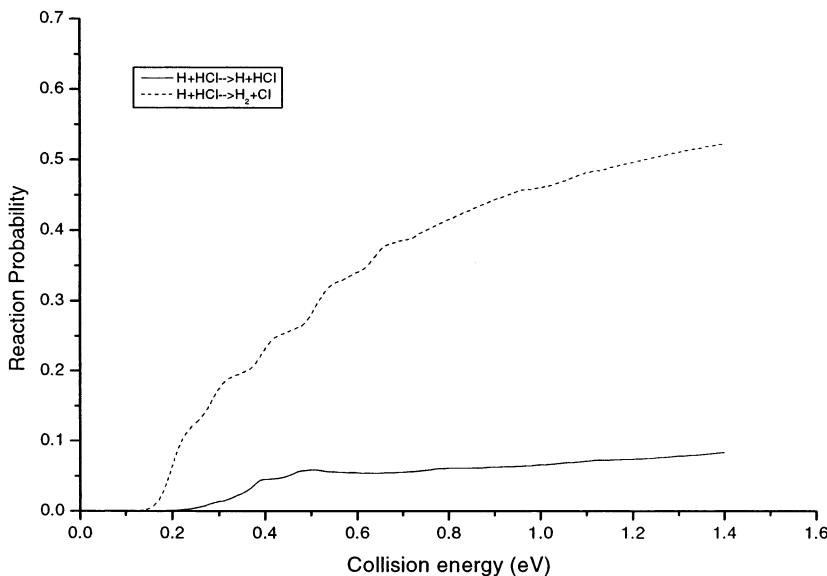


**Figure 1.** Total reaction probabilities for  $J = 0$  from the ground state of the HCl reactant for both channels of the H + HCl reaction on the BW2 PES. The solid line is for the exchange channel, and the dashed line is for the abstraction channel.

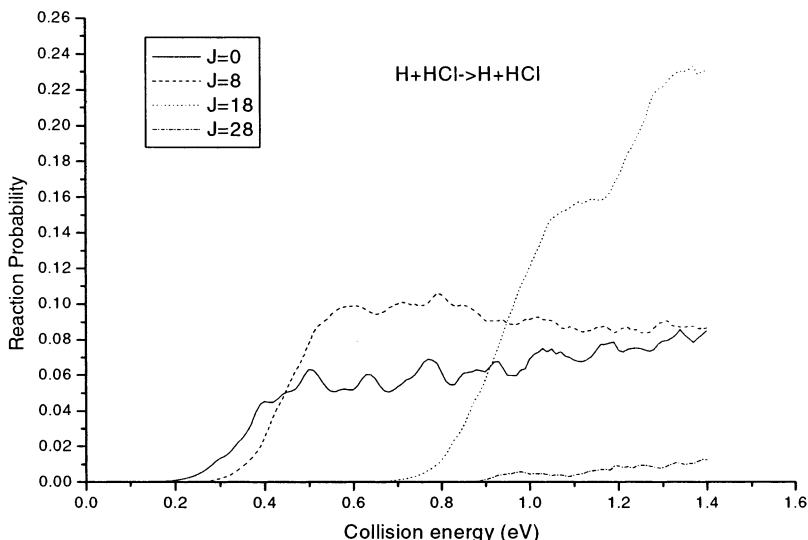


**Figure 2.** Total reaction probabilities for  $v = 0$ ,  $j = 0$ ,  $J = 0, 8, 18, 28$  of the HCl reactant for the exchange channel on the BW2 potential. The solid line is for  $J = 0$ , the dashed line is for  $J = 8$ , the dotted line is for  $J = 18$ , and the dashed-dotted line is for  $J = 28$ .

167 in the entire energy region, was achieved up to a few percent.  
 168 The initial wave packet was centered at  $R = 10a_0$ , with a width  
 169 of  $0.23a_0$  and an average translational energy of 0.8 eV.<sup>35</sup> For  
 170 lower  $J$ , we propagate the wave packets for 15000 au of time  
 171 to converge the low energy reaction probability (in all calculations,  
 172 a time step-size of 10 au was used). For  $J > 20$ , we  
 173 propagate the wave packets for a shorter time, because the  
 174 reaction probability in the low energy region is negligible.<sup>35</sup> In  
 175 this calculation, we used  $J$  from 0 to 80 to calculate the cross  
 176 section.

### 177 3. Results and Discussion

178 **Reaction Probabilities.** First of all, we computed the energy  
 179 resolved reaction probabilities for collision energies in the range  
 180 of [0.1, 1.4] eV with HCl initially in its ground state. The results  
 181 of  $J = 0$  as a function of the collision energy for the BW2  
 182 potential for all possible channels are presented in Figure 1. As  
 183 shown in Figure 1, the behavior of the reaction probabilities  
 184 for the two channels is quite different. One can see from Figure  
 185 1 that the reaction probability for the abstraction channel is much  
 186 higher than that of the exchange channel.

187 In the entrance channel of the  $H + HCl \rightarrow H_2 + Cl$  reaction,  
 188 a van der Waals (vdW) well with a collinear geometry and a  
 189 depth of 0.019 eV is found, while in the exit channel, a T-shaped  
 190 vdW well with a depth of 0.022 eV is predicted.<sup>28</sup> In the  
 191 collinear transition state for the abstraction reaction, the heights  
 192 of the classical barriers is 0.184 eV for BW2 PES.<sup>28</sup> For the  
 193  $H + ClH$  exchange reaction, which also has a collinear transition  
 194 state, the barrier height is computed to be 0.776 eV for BW2  
 195 PES.<sup>28</sup> The threshold of the reaction for the exchange channel  
 196 is a bit higher than that of the abstraction channel. This can  
 197 explain why the two channels show different behavior in  
 198 Figure 1.

199 In addition, we calculated the reaction probabilities for  
 200 different total angular momentum  $J$  for HCl initially in its ground  
 201 state. The reaction probabilities as a function of collision energy  
 202 for total angular momentum of  $J = 0, 8, 18$  and  $28$ , are presented  
 203 for both channels in Figure 2 and 3. As shown in Figure 2,  
 204 generally the values of the reaction probabilities decrease with  
 205 an increase of  $J$  in the low energy region. However, this is not  
 206 always true. For example, the  $J = 8, 18$  reaction probabilities  
 207 exceed the  $J = 0$  probability at high energies ( $> 0.45$  and

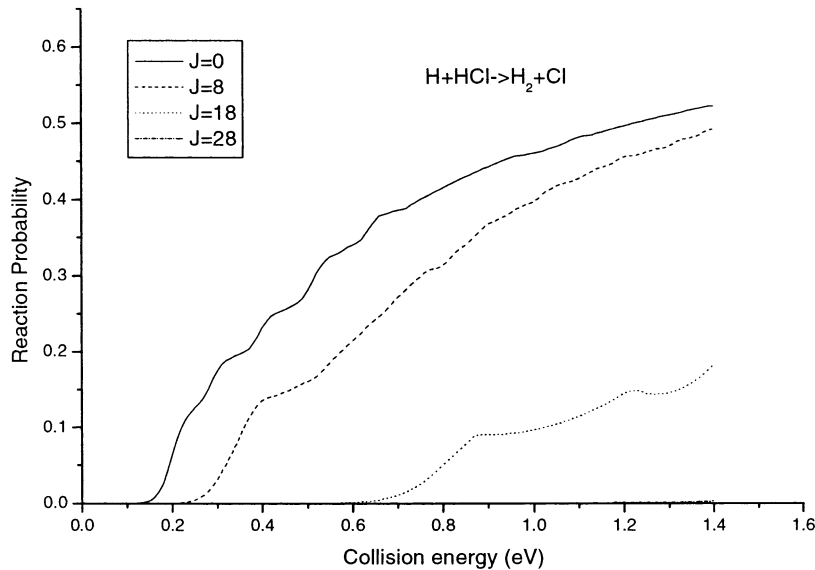


**Figure 3.** Total reaction probabilities for  $v = 0, j = 0, J = 0, 8, 18, 28$  of the HCl reactant for the abstraction channel on the BW2 potential. The solid line is for  $J = 0$ , the dashed line is for  $J = 8$ , the dotted line is for  $J = 18$ , and the dashed-dotted line is for  $J = 28$ .

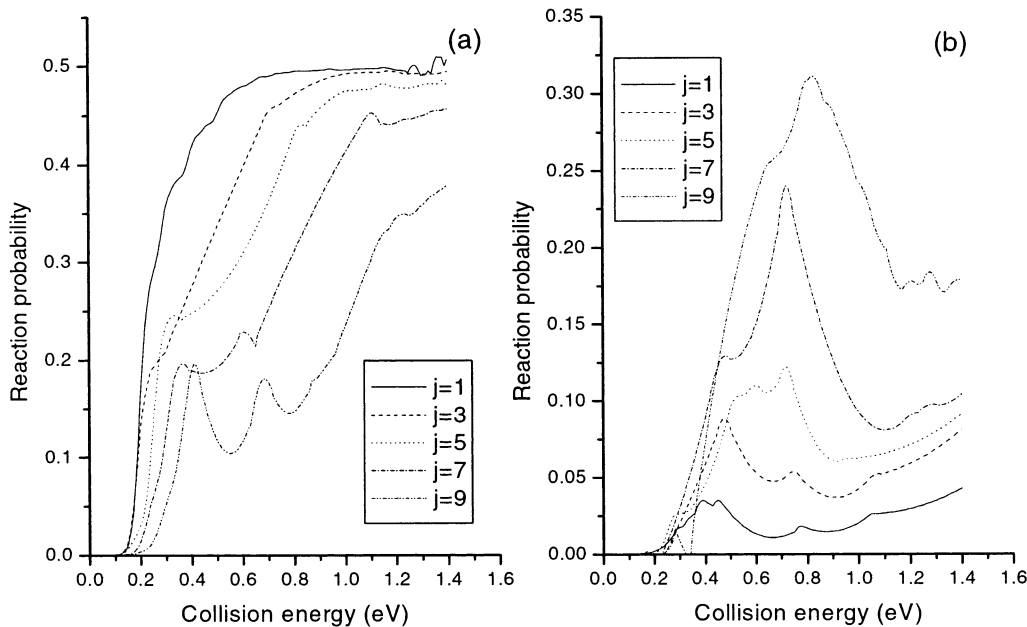


**Figure 4.** Total reaction probabilities for  $J = 0, v = 0$  of the HCl reactant for  $H + \text{HCl} \rightarrow H + \text{HCl}$  (a)  $H + \text{HCl} \rightarrow H_2 + \text{Cl}$  (b) on the BW2 potential. The solid line is for  $j = 1$ , dashed line is for  $j = 3$ , dotted line is for  $j = 5$ , dashed-dotted line is for  $j = 7$ , dashed-dotted-dotted line is for  $j = 9$ .

>0.9 eV), see Figure 2, while the values of the reaction probabilities for the abstraction channel decrease with an increase of  $J$  as shown in Figure 3. The threshold of the probabilities increases with increasing  $J$  in both channels.

The effect of the initial reagent rotation excitation on the reaction probability for the two channels ( $J = 0, v = 0, j = 1, 3, 5, 7, 9$ ) is shown in Figure 4. As seen from Figure 4, the reaction probabilities of the abstraction channel decrease with increasing rotational quantum number  $j$ . The decrease may be due to shape resonances caused by hydrogen tunneling through a centrifugal barrier, which traps the hydrogen for a finite time. The reaction probabilities for the exchange channel increase with increasing  $J$ . The increase and the oscillating can perhaps be explained by a long-range vdW well in both the entrance and exit channels that is the same as the explanation in ref 12. The oscillating of the probabilities turns stronger as  $j$  increases for the exchange channel.<sup>31</sup> The negative values of the reaction

probabilities in the low energy region is negligible with the approximate of the theory.

**Integral Cross Sections.** Next, we calculate the integral cross section from the initial ground state of HCl on the BW2 surface. In ref 30, Aoiz and Bañares carried out QCT calculation of the reaction cross section on the BW2 PES with HCl initially in its state ( $v = 0, j = 0-6$ ). The calculated cross sections for  $H + \text{HCl}$  are depicted in Figure 5 for both channels. As can be seen, the present cross section in the abstraction channel is systematically larger than the results of QCT<sup>30</sup> and the corresponding experimental values. For the exchange channel, the results from the QCT calculations cross with the ones from the TDWP calculations at 1.2 eV, and the threshold energy of the QCT results is much higher than the one from this work. The threshold energy of the TDWP results is much lower than the reaction barrier for this channel (0.8 eV). This can be explained by the fact that the TDWP method has correctly included the

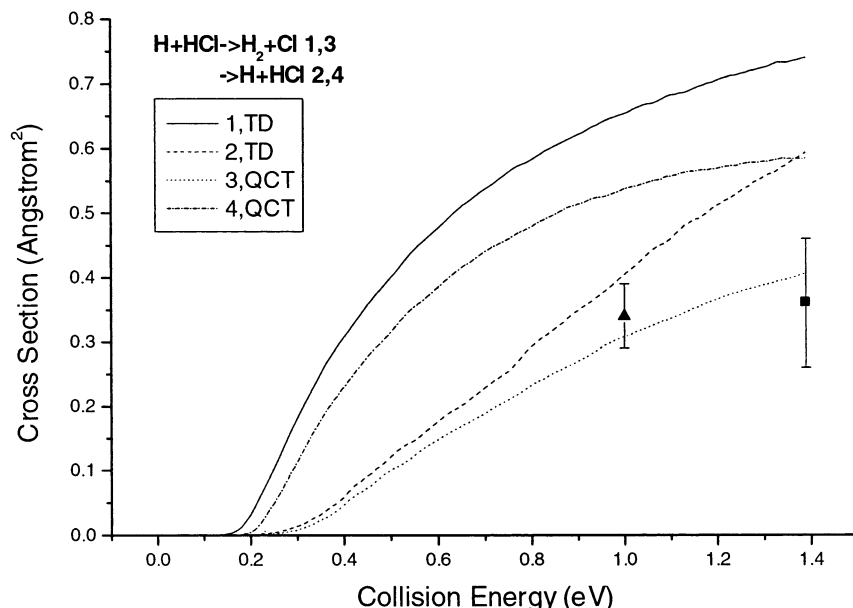


**Figure 5.** Reaction Cross section as a function of collision energy for the H + HCl reaction using TDWP approach and QCT on the BW2 PES. The results of the experimental measurements filled triangle of ref 36 and filled square of ref 16 as well as QCT excitation function calculated on the BW2 PES are also shown for comparison of the abstraction channel. The solid line and the dashed line are separately calculated for the abstraction channel and the exchange channel using the TDWP approach. The dotted line and the dashed-dotted line are in the results for the abstraction channel and exchange channel from QCT calculations. No experimental cross sections have been reported for the exchanged channel of the reaction.

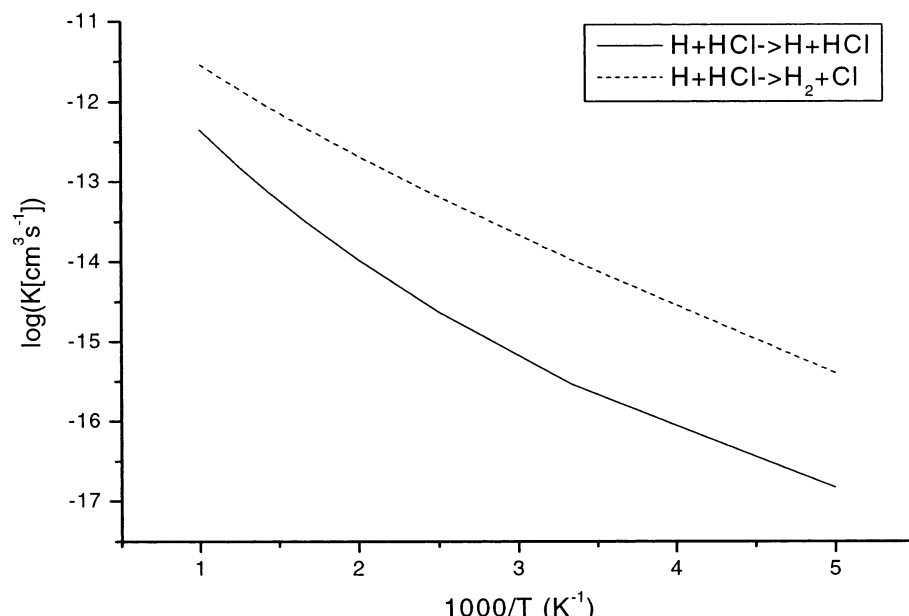


**Figure 6.** The Rate Constant for  $v = 0, j = 0$  of the HCl reactant for the H + HCl reaction eq I on the BW2 potential. The solid line represents the exchange channel, and the dashed line represents the abstraction channel.

zero-point energy and tunneling effects. Total absolute reaction cross sections for chlorine atom information,  $\sigma_R(1.4 \text{ eV}) = (0.35 \pm 0.16) \text{ Å}^2$ , have been measured using a photolytic calibration method.<sup>30</sup> In ref 25, a value of  $\sigma_R(1.0) = (0.34 \pm 0.05) \text{ Å}^2$  was determined employing vacuum-UV laser-induced fluorescence for Cl atom detection. However, in any case, the agreement is only approximate, because the BW2 cross sections lie outside the experimental points. The experimental values of  $(2 \pm 1) \text{ Å}^2$  reported in ref 9 for Ecol = 1.6 eV was not included in Figure 5.

At low temperature and collision energies, the tunneling works most remarkably in the reaction process to make the H abstraction easier. At high collision energies, the H atom has more chances to collide with the Cl atom, and the reaction will

produce more HCl; therefore, the result for the exchange channel increases faster than the one for the abstraction channel. It is surprising that dynamical calculations on the BW2 PES, which is based on high-quality ab initio points and clearly more accurate than any previous PES,<sup>28</sup> yield reaction cross sections for the abstraction channel noticeably larger than the experimental ones.<sup>30</sup> No experimental cross sections have been reported for the exchanged channel of the reaction.<sup>30</sup>

**Rate Constant.** Despite several measurements of relative reaction rates, accurate results for absolute rate constants have dodged investigators for many years. So, the rate constant calculations are also one of our main objectives.

One has to calculate the total reaction probability for more than two values of  $J$  to obtain a more accurate rate constant.<sup>32</sup>

270 A very accurate rate constant can be obtained by using reaction  
 271 probabilities evaluated at more than 6 values of  $J$  (partial waves).  
 272 The HCl initially in its state ( $v = 0, j = 0$ ) had been considered  
 273 in the calculation of  $K(T)$ .

274 The calculated rate constants for the H + HCl reaction are  
 275 depicted in Figure 6 for both channels. The calculation of the  
 276 thermal rate constants is in the range of temperatures between  
 277 200 and 1000 K. One can see that the calculated rate constant  
 278 of the abstraction channel is systematically larger than that of  
 279 the exchange channel for all the temperatures. As can be seen,  
 280 the present rate constants roughly follow the same as the  
 281 corresponding experimental values in the range of  $[10^{-17}, 10^{-12}]$   
 282  $\text{cm}^3\text{s}^{-1}$ .<sup>2,26,27,39-41</sup> However, in any case, the agreement is only  
 283 approximate, because the rate constants on BW2 PES lie inside  
 284 the range of experimental values. The agreement of the results  
 285 is presented here, and the experimental results are good enough,  
 286 but the BW2 PES need improvement of the theoretical results.

287 The calculated rate constant can also be taken as an indication  
 288 that the existence of quantum effects such as tunneling effect  
 289 may play an important role. So, according to our calculation  
 290 results here, possible reasons for the nonlinear behavior of the  
 291 Arrhenius plots of the reactions should be the combination  
 292 influence of tunneling effects.

293 One can predict that the rate constants of the exchange  
 294 channel from calculated reaction probabilities should also be  
 295 smaller. This feature is usually found for exothermic reactions  
 296 with a low energy barrier.<sup>42,43</sup>

#### 297 4. Conclusions

298 In this work, we have applied the TDWP approach to study  
 299 the H + HCl reaction on the BW2 PES. We have investigated  
 300 the reaction probabilities as a function of the collision energy  
 301 for the both channels for the H + HCl reaction and studied the  
 302 influence of the initial rotational state excitation of the reagents.  
 303 In the low temperature and collision energy range, the tunneling  
 304 works most remarkably in the reaction process to make the H  
 305 abstraction easier. In the high temperature and collision energy  
 306 region, the H atom has more chances to collide with the Cl  
 307 atom, and the reaction will produce more HCl. Thus, the cross  
 308 section for exchange channel increases faster than that of  
 309 abstraction channel. Such a study provides a clear and simple  
 310 picture about reaction mechanisms.

311 **Acknowledgment.** This work is supported by NSFC (Grants  
 312 Nos. 29825107 and 29853001) and NKBRSF.

#### 313 References and Notes

314 (1) See, e.g., (a) Allison, T. C.; Mielke, S. L.; Schwenke, D. W.; Lynch,  
 315 G. C.; Gordon, M. S.; Truhlar, D. G. In *Gas-Phase Chemical Reaction  
 316 System: Experiments and Models 100 Years after Max Bodenstein*, Springer  
 317 Series in Chemical Physics; Wolfrum, J., Volpp, H.-H., Rannacher, R.,  
 318 Warnatz, J., Eds.; Springer: Heidelberg, 1996; Vol. 61. (b) Aoiz, F. J.;  
 319 Bañares, L.; Herrero, V. J. *J. Chem. Soc., Faraday Trans.* **1998**, *94*, 2483,  
 320 and references therein.  
 321 (2) Miller, J. C.; Gordon, R. J. *J. Chem. Phys.* **1983**, *78*, 3713, and  
 322 references therein.  
 323 (3) See, e.g., (a) Clyne, M. A. A.; Stedman, D. H. *Trans. Faraday Soc.* **1966**, *62*, 2164. (b) Westenberg, A. A.; DeHaas, N. *J. Chem. Phys.*  
 324 **1968**, *48*, 4405. (c) Adusei, G. Y.; Fontijn, A. J. *Phys. Chem.* **1993**, *97*,  
 325 1409. (d) Atkinson, R.; Baulch, D. L.; Cox, R. A.; Hampson, R. F., Jr.;  
 326 Kerr, J. A.; Rossi, M. J.; Troe, J. *J. Phys. Chem. Ref. Data* **1997**, *26*, 521,  
 327 and references therein.

328 (4) Leone, S. R.; Moore, C. B. *Chem. Phys. Lett.* **1973**, *19*, 340. 329  
 329 (5) Wilkins, R. L. *J. Chem. Phys.* **1975**, *63*, 534. 330  
 330 (6) Wolfrum, J. In *Reactions of Small Transient Species*; Fontijn, A.,  
 331 Clyne, M. A. A., Eds.; Academic Press: New York, 1983. 332  
 332 (7) Miller, J. C.; Gordon, R. J. *J. Chem. Phys.* **1983**, *78*, 3713, and  
 333 references therein. 334  
 334 (8) Mielke, S. L.; Lynch, G. C.; Truhlar, D. G.; Schwenke, D. W. *J.  
 335 Phys. Chem.* **1994**, *98*, 8000. 335  
 335 (9) Aker, P. M.; Germann, G. J.; Valentini, J. *J. Chem. Phys.* **1989**,  
 336 *90*, 4795. 337  
 337 (10) Aker, P. M.; Germann, G. J.; Tabor, K. D.; Valentini, J. *J. Chem.  
 338 Phys.* **1989**, *90*, 4809. 338  
 338 (11) Wight, C. A.; Magnotta, F.; Leone, S. R. *J. Chem. Phys.* **1984**, *81*,  
 339 3951. 341  
 341 (12) Yang, B. H.; Gao, H. T.; Han, K. L.; Zhang, J. Z. H. *J. Chem.  
 343 Phys.* **2000**, *113*, 1434. 344  
 344 (13) Yang, B. H.; Yin, H. M.; Han, K. L. *J. Phys. Chem.* **2000**, *104*,  
 345 10517. 346  
 346 (14) Lin, S. Y.; Han, K. L.; Zhang, J. Z. H. *Chem. Phys. Lett.* **2000**,  
 347 *324*, 122. 348  
 348 (15) Kosloff, R. *J. Phys. Chem.* **1988**, *92*, 2087. 349  
 349 (16) Zhang, J. Z. H.; Dai, J.; Zhu, W. *J. Phys. Chem.* **1997**, *A101*, 2746,  
 350 and references therein. 351  
 351 (17) Neuhauser, D.; Baer, M.; Judson, R. S.; Kouri, D. J. *J. Chem. Phys.*  
 352 **1990**, *93*, 312. Judson, R. S.; Kouri, D. J.; Neuhauser, D.; Baer, M. *Phys.  
 353 Rev.* **1990**, *A42*, 351. 354  
 354 (18) Zhang, Y. C.; Zhan, L. X.; Zhang, Q. G.; Zhu, W.; Zhang, J. Z. H.  
 355 *Chem. Phys. Lett.* **1999**, *300*, 27. 356  
 356 (19) Zhang, D. H.; Zhang, J. Z. H. *J. Chem. Phys.* **1993**, *99*, 5615; **1994**,  
 357 *100*, 2697. 358  
 358 (20) Neuhauser, D. *J. Chem. Phys.* **1994**, *100*, 9272. 359  
 359 (21) Sato, S. *J. Chem. Phys.* **1955**, *23*, 2465. 360  
 360 (22) Zhu, W.; Dai, J.; Zhang, J. Z. H. *J. Chem. Phys.* **1996**, *105*, 4881.  
 361 Dai, J.; Zhu, W.; Zhang, J. Z. H. *J. Phys. Chem.* **1996**, *100*, 13901. 362  
 362 (23) Zhang, D. H.; Light, J. C. *J. Chem. Phys.* **1996**, *104*, 4544; **1996**,  
 363 *105*, 1291. 364  
 364 (24) Barclay, V. J.; Collings, B. A.; Polanyi, J. C.; Wang, J. H. *J. Phys.  
 365 Chem.* **1991**, *95*, 2921. 366  
 366 (25) Brownsword, R. A.; Kappel, C.; Schmiechen, P.; Upadhyaya, H.  
 367 P.; Volpp, H. R. *Chem. Phys. Lett.* **1998**, *289*, 241. 368  
 368 (26) Baer, M.; Last, I.; In *Potential Energy Surface and Dynamics  
 369 Calculations*; Truhlar, D. G., Ed.; Plenum Press: New York, 1981. 370  
 370 (27) Schwenke, D. W.; Tucker, S. C.; Steckler, R.; Brown, F. B.; Lynch,  
 371 G. C.; Truhlar, D. G.; Garrett, B. C. *J. Chem. Phys.* **1989**, *90*, 3110. 372  
 372 (28) Bian, W.; Werner, H.-J. *J. Chem. Phys.* **2000**, *112*, 220, and  
 373 references therein. 374  
 374 (29) Manthe, U.; Bian, W.; Werner, H.-J. *Chem. Phys. Lett.* **1999**, *313*,  
 375 647. 376  
 376 (30) Aoiz, F. J.; Bañares, L.; Bohm, T.; Hanf, A.; Herrero, V. J.; Jung,  
 377 K.-H.; Läuter, A.; Lee, K. W.; Menéndez, M.; Sáez Rábano, V.; Tamarro,  
 378 I.; Volpp, H.-R.; Wolfrum, J. *J. Phys. Chem.* **2000**, *104*, 10452. 379  
 379 (31) Aoiz, F. J.; Bañares, L.; Diez-Rojo, T.; Herrero, V. J.; Rábano,  
 380 V. S. *J. Phys. Chem.* **1996**, *100*, 4071. 381  
 381 (32) Zhang, D. H.; Zhang, J. Z. H. *J. Chem. Phys.* **1999**, *110*, 7622. 382  
 382 (33) (a) Sun, Q.; Bowman, J. M.; Schatz, G. C.; Sharp, J. R.; Connor,  
 383 J. N. L. *J. Chem. Phys.* **1990**, *92*, 1677. (b) Bowman, J. M. *J. Phys. Chem.*  
 384 **1991**, *95*, 4960. 385  
 385 (34) Zhang, D. H.; Zhang, J. Z. H. *J. Chem. Phys.* **1994**, *101*, 3671.  
 386 Dai, J.; Zhang, J. Z. H. *J. Phys. Chem.* **1996**, *100*, 6898. 387  
 387 (35) Zhang, D. H.; Lee, S.-Y.; Baer, M. *J. Chem. Phys.* **2000**, *112*, 9802.  
 388 (36) Fleck, J. A.; Morris, J. R., Jr.; Feit, M. D. *Appl. Phys.* **1976**, *10*,  
 389 129. 390  
 390 (37) Neuhauser, D.; Baer, M. *J. Chem. Phys.* **1989**, *91*, 4651. 391  
 391 (38) Zhang, D. H.; Zhang, J. Z. H. *J. Chem. Phys.* **1994**, *101*, 1146. 392  
 392 (39) Aker, P. M.; Germann, G. J.; Polanyi, J. C.; Wang, J. H. *J. Phys.  
 393 Chem.* **1991**, *95*, 2921. 394  
 394 (40) Stouteris, D.; Manolopoulos, D. E.; Bian, W.; Werner, H.-J.; Lai,  
 395 L.-H.; Liu, K. *Science* **1999**, *286*, 1713. 396  
 396 (41) Sathyamurthy, N. *Chem. Rev.* **1983**, *83*, 601. Zhu, W.; Zhang, J.  
 397 Z. H.; Zhang, Y. C.; Zhang, Y. B.; Zhan, L. X.; Zhang, S. L.; Zhang, D. H.  
 398 *J. Chem. Phys.* **1998**, *108*, 3509. Zhu, W.; Zhang, J. Z. H.; Zhang, D. H.  
 399 *Chem. Phys. Lett.* **1998**, *292*, 46. 400  
 400 (42) Zhu, W.; Wang, D. Y.; Zhang, J. Z. H. *Theor. Chem. Acc.* **1997**,  
 401 *96*, 31. 402  
 402 (43) Tang, B. Y.; Yang, B. H.; Han, K. L.; Zhang, R. Q.; Zhang, J. Z.  
 403 *J. Chem. Phys.* **2000**, *113*, 10105. 404